Dual role of Fe dopants in enhancing stability and charge transfer in (Li_{0.8}Fe_{0.2})OHFeSe superconductors

Wei Chen, Changgan Zeng, Efthimios Kaxiras, and Zhenyu Zhang

Phys. Rev. B **93**, 064517 — Published 25 February 2016

DOI: 10.1103/PhysRevB.93.064517

The Dual Role of Fe Dopants in Enhancing Stability and Charge Transfer in $(Li_{0.8}Fe_{0.2})$OHFeSe Superconductors

Wei Chen,[1,2] Changgan Zeng,[1] Efthimios Kaxiras,[2] and Zhenyu Zhang[1,*]

[1] *International Center for Quantum Design of Functional Materials (ICQD), Hefei National Laboratory for Physical Sciences at Microscale, and Synergetic Innovation Center of Quantum Information and Quantum Physics, University of Science and Technology of China, Hefei, Anhui 230026, China*

[2] *Department of Physics and School of Engineering and Applied Sciences, Harvard University, Cambridge, Massachusetts 02138, USA*

(Dated: February 8, 2016)

The recently discovered $(Li_{0.8}Fe_{0.2})$OHFeSe superconductor provides a new platform for exploiting the microscopic mechanisms of high-T_c superconductivity in FeSe-derived systems. Using density functional theory calculations, we first show that substitution of Li by Fe not only significantly strengthens the attraction between the $(Li_{0.8}Fe_{0.2})$OH spacing layers and the FeSe superconducting layers along the c axis, but also minimizes the lattice mismatch between the two in the ab plane, both favorable for stabilizing the overall structure. Next we explore the electron injection into FeSe from the spacing layers, and unambiguously identify the $Fe_{0.2}$ components to be the origin of the dramatically enhanced interlayer charge transfer. We further reveal that the system strongly favors collinear antiferromagnetic ordering in the FeSe layers, but the spacing layers can be either antiferromagnetic or ferromagnetic depending on the $Fe_{0.2}$ spatial distribution. Based on these insights, we predict $(Li_{0.8}Co_{0.2})$OHFeSe to be structurally stable with even larger electron injection and potentially higher T_c.

PACS numbers: 74.70.-b, 74.62.Dh, 74.25.Ha, 84.30.Bv

Recently, two groups discovered $(Li_{1-x}Fe_x)$OHFeSe ($x \sim 0.2$) as a new class of superconductors with high superconducting transition temperatures (T_c), and demonstrated coexistence of superconductivity and antiferromagnetism (AFM) or ferromagnetism (FM) in these systems [1, 2]. Such systems provide several appealing features for revealing the superconducting mechanisms [1–4]. Subsequent experimental studies have confirmed the essential role of the spacing layers [3–7], but there is little understanding of how useful the dopant Fe_x atoms are in obtaining superconducting behavior. A key, as yet unanswered, mystery is the magnetic ordering in the spacing layers, especially since the indications from the two pioneering experiments are inconsistent with each other [1, 2]. Overall, it is highly desirable to understand two key features of these systems: (i) the structural stability of weakly interacting spacers and superconducting FeSe monolayers [1, 2]; (ii) the atomic origin of the electron doping from the $(Li_{1-x}Fe_x)$OH layers. Insights into those important issues will facilitate the search for new FeSe-based superconductors with potentially higher T_c.

In this Letter, we use density functional theory (DFT) calculations with the VASP code [8] to investigate the dominant roles of the spacers in establishing the high-T_c superconductivity of $(Li_{0.8}Fe_{0.2})$OHFeSe, with particular emphasis on the $Fe_{0.2}$ atoms. We find that substitution of Li by Fe enhances the structural stability both in the ab plane and along the c axis. By further exploring the charge transfer, we identify the $Fe_{0.2}$ atoms to be the origin of significant electron injection into FeSe. In addition, we obtain the ground-state magnetic order, and explain the seemingly contradictory experimental observations on the magnetic ordering of the spacing layers. Based on these findings, we predict a stable $(Li_{0.8}Co_{0.2})$OHFeSe structure with larger electron doping into FeSe, potentially resulting in an even higher T_c.

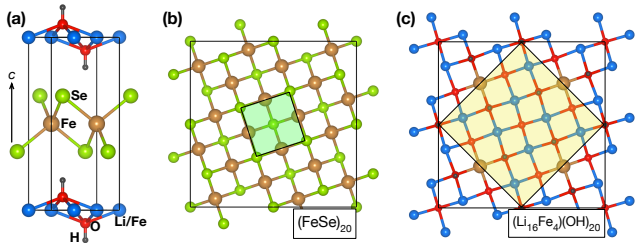

FIG. 1. (a) Side view of the 1×1 (Li/Fe)OHFeSe, and top views of: (b) the FeSe, and (c) the $(Li_{0.8}Fe_{0.2})$OH layer in a $\sqrt{10} \times \sqrt{10}$ cell. The green shaded area is the 1×1 cell, while the yellow one is the $\sqrt{5} \times \sqrt{5}$ cell, which is compatible with states of nonmagnetic (NM), FM, or checkerboard AFM order in FeSe. The collinear AFM order in FeSe requires an expanded cell of $\sqrt{10} \times \sqrt{10}$.

We first perform lattice-constant relaxation of $(Li_{0.8}Fe_{0.2})$OHFeSe with different functionals and van der Waals (vdW) approaches, in order to choose the proper theoretical framework that can describe the systems under investigation here [9]. In constructing the supercells, we followed two considerations: (1) $(Li_{0.8}Fe_{0.2})$OH layers have an occupation of Li/Fe with a ratio of ~ 4 [1], and thus the smallest cell is $\sqrt{5} \times \sqrt{5}$; (2) as discussed explicitly below, the ground-state magnetic order is found to be

collinear AFM for FeSe, consistent with several previous studies of the FeSe/$SrTiO_3$ (FeSe/STO) system [10–12]. Therefore, a $\sqrt{10}\times\sqrt{10}$ cell is used to optimize the lattice parameters of the ground-state $(Li_{0.8}Fe_{0.2})$OHFeSe structure. Figs. 1b and 1c display the atomic structures of the FeSe and $(Li_{0.8}Fe_{0.2})$OH layers. We first considered the $Fe_{0.2}$ atoms in the spacer to be orderly distributed, forming a square lattice with the nearest-neighbor Fe-Fe distance constant. We then relaxed this restriction, but found that the clustering or disordering of the $Fe_{0.2}$ atoms is energetically less favorable [9].

TABLE I. Calculated lattice constants of $(Li_{0.8}Fe_{0.2})$OHFeSe and LiOHFeSe. The vdW methods are based on the PBE functional. Numbers are in units of Å. These results are obtained from optimization of the $\sqrt{10}\times\sqrt{10}$ cells, and the data is normalized to the 1×1 cells.

	$(Li_{0.8}Fe_{0.2})$OHFeSe					LiOHFeSe
EXP[a]	non-vdW		vdW			non-vdW
	LDA	PBE	DFT-D2	DFT-TS	vdW-DF2	PBE
a = 3.786	FTE[b]	3.79	3.72	3.69	FTE[b]	3.68
c = 9.288	< 8.20	9.38	8.52	8.30	> 9.78	11.16

[a] EXP: experimental data at room temperature [1].
[b] FTE: fixed to the experimental value.

The optimized lattice parameters are shown in Table I, calculated from the energy dependence on the lattice constants. The magnetic spin texture was simultaneously optimized, and the ground-state magnetism will be discussed below in Figure 3. For LDA and vdW-DF2, we first fixed a to the experimental value [1], and found a large deviation in the value of c from the experimental one. For the rest, a and c were optimized simultaneously to convergence. Between the non-vdW approaches, LDA significantly underestimates the lattice constants while PBE slightly overestimates them, as commonly found for the two functionals. The implemented vdW corrections as the empirical pairwise forms of C_6/R_0^6 [13, 14] in DFT-D2 and DFT-TS are found to over-compensate the correction to c; more surprisingly, the non-local vdW functional [15–17] included in vdW-DF2 is found to severely overestimate c. The failures of these vdW methods may originate from the excessively large C_6 coefficients due to the neglect of screening and many-body effects in the first two functionals, and from the imprecise exchange functional in the latter. These problems call for in-depth investigations and possibly require major improvements in the methodology. Presently, given the relatively small errors (a: +0.16%, c: +0.96%), we conclude that the PBE functional without including either of the popular vdW corrections yields a reasonable description, and thus the following results are all based on this approach.

To determine the role of $Fe_{0.2}$ in the structural properties, we calculate the lattice constants of LiOHFeSe. With the Fe atoms removed from the spacer, the collinear AFM order is calculated to persist in the FeSe layer. The obtained value (Table I) for a is reduced by 3.01% and for c is enlarged by 19.01% compared to the lattice constants of $(Li_{0.8}Fe_{0.2})$OHFeSe calculated by PBE. In the following, we analyze the effects on the lattice parameters in more detail.

Experimentally, FeSe is found to be compressed in the ab plane of $(Li_{0.8}Fe_{0.2})$OHFeSe [1], where intuitively the strain should be caused by the smaller lattice of $(Li_{0.8}Fe_{0.2})$OH. Based on our results, the $Fe_{0.2}$ atoms indeed have expanded the ab lattice; otherwise, the spacer could be even smaller in ab, and the ensuing larger mismatch with FeSe would make it unlikely to form a stable intercalated structure. To confirm this conjecture, we further calculate the lattice parameters of FeSe, $(Li_{0.8}Fe_{0.2})$OH, and LiOH monolayers separately, and find their a values to be 3.74 Å, 3.73 Å, and 3.59 Å, respectively. These values, together with that of bulk $(Li_{0.8}Fe_{0.2})$OHFeSe, suggest that thinking of FeSe as being compressed in the plane [1] may be inaccurate; however, our conjecture remains valid, given the small (*or* large) lattice mismatch between FeSe and $(Li_{0.8}Fe_{0.2})$OH (*or* LiOH). We conclude that the $Fe_{0.2}$ atoms play a vital role in minimizing the lattice mismatch between the spacer and FeSe, which enables the formation of the *commensurate stacking* as shown in Fig. 1a.

The FeSe and $(Li_{0.8}Fe_{0.2})$OH layers are both stretched slightly in the plane to a common lattice constant of 3.79 Å when they are stacked alternatingly. This seems counter-intuitive, as the interface generally adopts an intermediate lattice constant. Here since we use the free-standing monolayers as the reference, this observation is very likely to be caused by the interlayer bonding between the FeSe and $(Li_{0.8}Fe_{0.2})$OH layers along the c direction. Next we further examine the structures by calculating the thickness d of each layer, defined as the distance from the upper Se *or* H to the lower Se *or* H position along the c direction for the FeSe monolayer *or* $(Li_{0.8}Fe_{0.2})$OH spacing layer. We find that d shrinks from 3.48 to 3.33 Å for $(Li_{0.8}Fe_{0.2})$OH, while it expands from 2.89 to 2.91 Å for FeSe, when the two layers are alternatingly assembled into a bulk structure. The volume expansion (from $3.74^2\times2.89 = 40.42$ to $3.79^2\times2.91 = 41.80$ Å^3) of FeSe suggests an increased Coulomb repulsion internally, which strongly indicates electron injection. The $(Li_{0.8}Fe_{0.2})$OH layer is found to be rippled, with an amplitude of ∼0.12 Å for H atoms differing from their average position along the c-axis, making its in-plane lattice relatively easy to be stretched by interacting with the expanded FeSe, and the thickness tends to decrease to compensate for this in-plane expansion. Combining all the dimensions, the volume shrinks (from $3.73^2\times3.48 = 48.42$ to $3.79^2\times3.33 = 47.83$Å^3), which is supposedly caused by electron depletion. It is worth noting that the subtle correlation between structural volume expansion and electron doping may have been neglected in other FeSe-based systems (such as FeSe/STO [18–24] and alkali-intercalated FeSe) that rely on charge transfer to enhance

T_c.

We now examine how the $Fe_{0.2}$ dopants influence the overall structures along the vertical directions. The c axis is reduced from 11.16 Å to 9.38 Å when the $Fe_{0.2}$ atoms are incorporated into the spacer. Such a dramatic change suggests a greatly enhanced attraction between the spacer and FeSe, which should have an immediate contribution to the in-plane expansion from 3.68 Å to 3.79 Å. A relevant quantity to calculate is the cohesive energy: $E_C = E_{FeSe} + E_{Spacer} - E_{Bulk}$, where E_{FeSe} is the total energy of the FeSe monolayer, E_{Spacer} is that of $(Li_{0.8}Fe_{0.2})OH$ (*or* LiOH), and E_{Bulk} is that of the combined bulk. E_{FeSe} and E_{Spacer} are calculated using the in-plane lattice of the corresponding bulk system. Our results show that, E_C per formula unit is 0.02 eV for LiOHFeSe and 0.35 eV for $(Li_{0.8}Fe_{0.2})$OHFeSe. For the former, the value is even smaller than E_C per carbon in graphite [25], and the average bond distance $\overline{d}$ of the nearest Se-H is 3.50 Å, clearly in the regime of weak vdW interaction. In contrast, for $(Li_{0.8}Fe_{0.2})$OHFeSe, E_C is stronger than that of vdW interaction, but still weaker than the typical strength of chemical bonding. This moderate interaction originating from the incorporated $Fe_{0.2}$ substantially stabilizes the structure in the vertical direction, while still allows mechanical cleavage of the crystal [4, 6, 7]. More importantly, such an increased E_C and the closer contact ($\overline{d}$ = 3.11 Å) between FeSe and $(Li_{0.8}Fe_{0.2})$OH together enable enhanced charge transfer between the layers.

Following the above structural indications, we next investigate the detailed nature of charge transfer. We calculate the charge density difference $\Delta\rho$ between the combined $(Li_{0.8}Fe_{0.2})$OHFeSe bulk system and the sum of the isolated FeSe and $(Li_{0.8}Fe_{0.2})$OH layers. To obtain a quantitative picture, we plot the plane-averaged $\Delta\rho$ along the c axis ($\Delta\rho_z$), shown in Fig. 2a. To understand the role of $Fe_{0.2}$, we also calculate $\Delta\rho_z$ for LiOHFeSe at the fixed lattice constant of $(Li_{0.8}Fe_{0.2})$OHFeSe and at the relaxed lattice, as shown in Figs. 2b and 2c respectively.

From this analysis, we find that when the $(Li_{0.8}Fe_{0.2})$OH and FeSe layers merge into the bulk structure, the charge density between Fe and Se in FeSe has an electron-depletion region, and this amount of charge is mostly transferred to the Se planes to form interactions with the spacers. Such features are not observed in LiOHFeSe, where the interlayer E_C is much weaker. In each plot, we shift the average z position of the Fe atoms in FeSe to be located exactly at the center of the supercell. The charge redistribution is mirror symmetric with respect to the middle line in Figs. 2a and 2b. However, in Fig. 2c, the layers are loosely stacked with the interlayer distance found to be slightly alternating (the distance between the Se and H planes differs by ∼0.15 Å at the two opposite sides of FeSe), making the curve not exactly symmetric. To see the

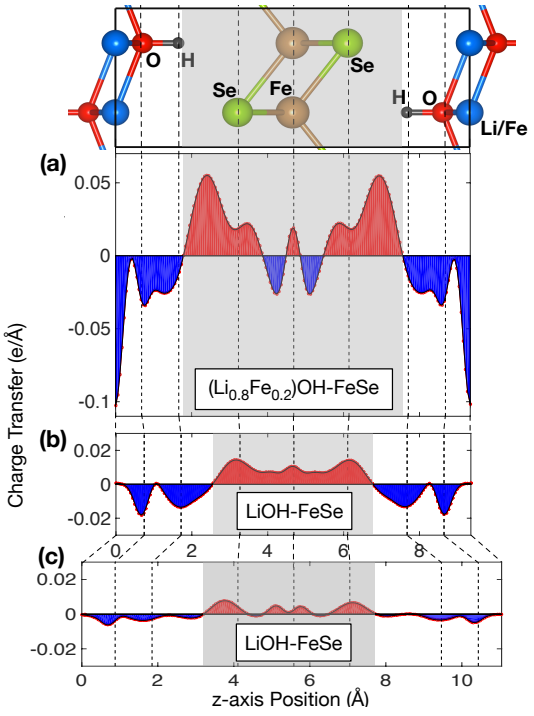

FIG. 2. $\Delta\rho_z$ of (a) $(Li_{0.8}Fe_{0.2})$OHFeSe and (b,c) LiOHFeSe at the lattice constant of $(Li_{0.8}Fe_{0.2})$OHFeSe and of LiOHFeSe. These results are calculated from the ground states of $\sqrt{10}\times\sqrt{10}$ cells, and have been normalized to 1×1 cells. The red and blue shaded areas indicate electron accumulation and depletion, respectively.

doping levels of FeSe, we integrate $\Delta\rho_z$ over z within the region of FeSe (the gray shaded areas in Fig. 2). The boundaries between Se and H are located at the positions where the signs of $\Delta\rho_z$ change. The electron injection ρ_I into FeSe is calculated to be 0.052 electrons per FeSe in $(Li_{0.8}Fe_{0.2})$OHFeSe. For LiOHFeSe, ρ_I = 0.019 e/Fe and 0.006 e/Fe for structures with the $(Li_{0.8}Fe_{0.2})$OHFeSe and LiOHFeSe lattice constants, respectively. The estimated value of 0.052 is close to the experimentally measured value of ∼0.08 e/Fe [3], and the difference might be due to the absence of structural defects or disordering of $Fe_{0.2}$ in the supercell systems.

From a broader perspective, a sufficiently large electron doping is essential to realize high T_c in FeSe-based superconductors. In the FeSe/STO systems, O vacancies in STO [26] are believed to be the origin of large interlayer charge transfer [27]. Here in $(Li_{0.8}Fe_{0.2})$OHFeSe, one may naturally think that the origin of electron injection is the $Fe_{0.2}$ atoms in the spacer, because of their generally higher oxidation state than Li. Indeed, our results agree with this conjecture, and demonstrate that the $Fe_{0.2}$ atoms enhance the electron injection into FeSe in two ways: First, by comparing Figs. 2a and 2b where the lattice constants are identical, we clearly see the large contribution of the $Fe_{0.2}$ d orbitals to the charge transfer

when Li is substituted; second, the increased doping in Fig. 2b compared to Fig. 2c indicates that the closer interlayer coupling caused by $Fe_{0.2}$ also boosts the amount of charge transfer. These two effects are crucial, and their identification should be a useful guide in the search for other novel spacer-intercalated superconductors.

The interlayer charge transfer results in the higher T_c in bulk $(Li_{0.8}Fe_{0.2})$OHFeSe than in bulk FeSe; however, the doping level of FeSe in $(Li_{0.8}Fe_{0.2})$OHFeSe is still lower than that in FeSe/STO [3], suggesting the possibility that other structural designs could further enhance T_c. Based on the above studies of the role of $Fe_{0.2}$, we can attempt to substitute Li by other elements instead of Fe in the spacers, to see if they stabilize the structure, and more importantly, if they can induce larger charge transfer. Presently, we have examined Mn or Co in the place of Fe, which potentially have higher oxidation state than that of Fe. Our calculations show that both $(Li_{0.8}Mn_{0.2})$OHFeSe and $(Li_{0.8}Co_{0.2})$OHFeSe are indeed structurally stable, with lattice constants similar to that of $(Li_{0.8}Fe_{0.2})$OHFeSe. E_C per formula unit is calculated to be 0.39 eV and 0.26 eV for $(Li_{0.8}Mn_{0.2})$OHFeSe and $(Li_{0.8}Co_{0.2})$OHFeSe, respectively. Furthermore, their charge-transfer curves have similar trend as that shown in Fig. 2a, and ρ_I is calculated to be $0.044e$/Fe for $(Li_{0.8}Mn_{0.2})$OHFeSe and $0.060e$/Fe for $(Li_{0.8}Co_{0.2})$OHFeSe. The Mn and Co atoms do not appear to contribute to the charge injection of FeSe as much as Fe, but significantly facilitate more electron transfer from the O atoms in the spacer. The depleted area in FeSe of $(Li_{0.8}Co_{0.2})$OHFeSe is also found to be smaller than that in $(Li_{0.8}Fe_{0.2})$OHFeSe. The larger ρ_I of $(Li_{0.8}Co_{0.2})$OHFeSe suggests a higher T_c than that of $(Li_{0.8}Fe_{0.2})$OHFeSe.

We next focus on the magnetic properties, as magnetism is generally related to superconductivity in the FeSe-derived systems. We examine four different magnetic orders in each of the FeSe and $(Li_{0.8}Fe_{0.2})$OH layers, including NM, FM, checkerboard AFM, and collinear AFM, and investigate their possible combinations for interlayer coupling. Our calculations show that FM order is unstable in FeSe, and NM order is unstable in $(Li_{0.8}Fe_{0.2})$OH. The computed magnetic moment of Fe in $(Li_{0.8}Fe_{0.2})$OH is $\sim 3.53\mu_B$, and in FeSe $\sim 2.25\mu_B$ in the collinear AFM order and $\sim 1.86\mu_B$ in the checkerboard AFM order. These DFT calculated local moments might be bigger than the corresponding moments measured by experiments, because of the magnetic fluctuation of the itinerant electrons. The larger moment of Fe in $(Li_{0.8}Fe_{0.2})$OH suggests that the spin magnitude of the Fe atoms in FeSe is reduced due to closer packing. By comparing the total energies of the different magnetically ordered states, we obtain the magnetic ground state of $(Li_{0.8}Fe_{0.2})$OHFeSe (Fig. 3). Both layers exhibit a collinear AFM order in the Fe square lattices, and the interlayer spins are aligned parallel to each other. We find AFM order to be slightly more stable than FM order by only 2 meV per Fe atom in $(Li_{0.8}Fe_{0.2})$OH. Such results of the fragile AFM ground state in the spacer also help explain the recent experimental observations [28]. In addition, of the systems proposed here as candidates for higher T_c, $(Li_{0.8}Co_{0.2})$OHFeSe has the same spin configuration as $(Li_{0.8}Fe_{0.2})$OHFeSe, while $(Li_{0.8}Mn_{0.2})$OHFeSe exhibits anti-parallel alignment between the collinear AFM FeSe and $(Li_{0.8}Mn_{0.2})$OH layers.

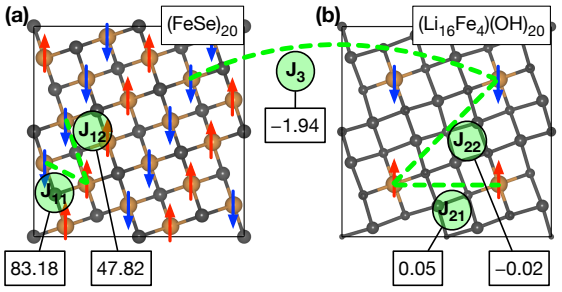

FIG. 3. Ground-state magnetism of $(Li_{0.8}Fe_{0.2})$OHFeSe in the (a) FeSe and (b) $(Li_{0.8}Fe_{0.2})$OH layers. Elements other than Fe have moments of ∼0, and are colored in gray. The green lines connect the nearest or next-nearest Fe neighbors, whose magnetic couplings are considered in the Heisenberg model. The values of coupling parameters are in units of meV/S^2.

Based on the total energies calculated from DFT, we quantitatively analyze the coupling strengths in $(Li_{0.8}Fe_{0.2})$OHFeSe using the Heisenberg model on square lattices [9]. Although this formalism is originally developed for insulating systems, it is also commonly used in itinerant magnetic systems, where the contributions to the magnetic couplings from itinerant electrons might be missed in the model. We use the approximate Hamiltonian:

$$H=[(J_{11}\sum_{<ij>}+J_{12}\sum_{\ll ij\gg})\vec{S}_i\cdot\vec{S}_j]_1+[(J_{21}\sum_{<ij>}+J_{22}\sum_{\ll ij\gg})\vec{S}_i\cdot\vec{S}_j]_2+[J_3\sum_{<ij>}\vec{S}_i\cdot\vec{S}_j]_3. \quad (1)$$

The three terms account for couplings in FeSe, in $(Li_{0.8}Fe_{0.2})$OH, and between the two layers, in this order. $<ij>$ and $\ll ij\gg$ represent summations over the nearest and next-nearest neighbors. From the energies of different magnetically ordered states, we estimate the coupling strengths shown in Fig. 3 [9]. We note that the computed J_{11} and J_{12} in FeSe are quite close to previous results [12, 29]. The order of the coupling strength is: $J_{11} > J_{12} \gg J_3 \gg J_{21} > J_{22}$, the reverse of the Fe-Fe pair distances ($d_{11} < d_{12} < d_3 < d_{21} < d_{22}$). The couplings in $(Li_{0.8}Fe_{0.2})$OH are quite weak, making its magnetic order dominated by the relatively larger coupling between the layers. The magnetic order of FeSe and the negative value of J_3 result in a collinear AFM ground state in $(Li_{0.8}Fe_{0.2})$OH (Fig. 3b), with the spin direction of each site parallel to that of the corresponding Fe in FeSe. Furthermore, the much weaker J_3 compared

to J_{11} and J_{12} suggests that $Fe_{0.2}$ should play a minimal role in directly influencing the magnetism of FeSe by magnetic coupling between the layers. This fact also indicates that the magnetic coupling between FeSe and the spacer is unlikely to play an important role, or probably even undesirable in establishing high T_c. The ground-state magnetic order described above is computed using an ordered distribution of $Fe_{0.2}$ atoms in the spacer. In the actual systems, a certain degree of disorder is unavoidable. This structural fact could possibly change the coupling strengths within the spacing layer as well as the Fe sites in FeSe that are closer to the $Fe_{0.2}$ atoms. By calculating the ground-state magnetic order, here we demonstrate that disordering of $Fe_{0.2}$ can possibly result in a FM order in the spacer [9]. This finding may help to clarify the controversial experimental observations of different magnetic orders in $(Li_{0.8}Fe_{0.2})OH$ [1, 2].

Despite the limitations inherent in our approach [9], our study reveals the dual role of $Fe_{0.2}$ dopants in the structural stability and in the electronic charge injection into FeSe. Both aspects are critically important in the fabrication of FeSe-based high-T_c superconductors and may provide new insights into exploration of the likely pairing mechanisms. Using these insights, we predict that $(Li_{0.8}Co_{0.2})OH$ superconductors will exhibit larger charge transfer and potentially higher T_c; although it is notable that Co substitution is common in FeSe which may reduce T_c, we hope this present study will stimulate experimental efforts to minimize (maximize) the Co concentration in the FeSe (spacing) layer, to validate our prediction.

We are grateful to Qiang Zhang, Wei Qin, Dennis Huang, and Shiang Fang for helpful discussions. This work was supported by the National Natural Science Foundation of China (Grant Nos. 61434002, 11204286, 11504357, and 11434009), the National Key Basic Research Program of China (Grant No. 2014CB921103), and the Fundamental Research Funds for the Central Universities (No. WK2030020027). The calculations were performed at National Energy Research Scientific Computing Center (NERSC) of the U.S. Department of Energy.

* zhangzy@ustc.edu.cn

[1] X. F. Lu, N. Z. Wang, H. Wu, Y. P. Wu, D. Zhao, X. Z. Zeng, X. G. Luo, T. Wu, W. Bao, G. H. Zhang, F. Q. Huang, Q. Z. Huang, and X. H. Chen, Nat. Mater. **14**, 325 (2015).

[2] U. Pachmayr, F. Nitsche, H. Luetkens, S. Kamusella, F. Brückner, R. Sarkar, H.-H. Klauss, and D. Johrendt, Angew. Chem. Int. Ed. **54**, 293 (2015).

[3] L. Zhao, A. Liang, D. Yuan, Y. Hu, D. Liu, J. Huang, S. He, B. Shen, Y. Xu, X. Liu, L. Yu, G. Liu, H. Zhou, Y. Huang, X. Dong, F. Zhou, Z. Zhao, G. Chen, Z. Xu, and X. J. Zhou, arXiv:1505.06361 (2015).

[4] X. H. Niu, R. Peng, H. C. Xu, Y. J. Yan, J. Jiang, D. F. Xu, T. L. Yu, Q. Song, Z. C. Huang, Y. X. Wang, B. P. Xie, X. F. Lu, N. Z. Wang, X. H. Chen, Z. Sun, and D. L. Feng, Phys. Rev. B **92**, 060504 (2015).

[5] B. Lei, Z. J. Xiang, X. F. Lu, N. Z. Wang, J. R. Chang, C. Shang, X. G. Luo, T. Wu, Z. Sun, and X. H. Chen, arXiv:1503.02457 (2015).

[6] Y. J. Yan, W. H. Zhang, M. Q. Ren, X. Liu, X. F. Lu, N. Z. Wang, X. H. Niu, Q. Fan, J. Miao, R. Tao, B. P. Xie, X. H. Chen, T. Zhang, and D. L. Feng, arXiv:1507.02577 (2015).

[7] Z. Du, X. Yang, H. Lin, D. Fang, G. Du, J. Xing, H. Yang, X. Zhu, and H.-H. Wen, arXiv:1506.04645 (2015).

[8] G. Kresse and J. Furthmüller, Phys. Rev. B **54**, 11169 (1996).

[9] See Supplemental Materials for details on the methods of DFT calculations employed, the dependence of the energy and magnetic order on the $Fe_{0.2}$ distribution, the calculations of magnetic coupling parameters, and the limitations of the present study.

[10] F. Zheng, Z. Wang, W. Kang, and P. Zhang, Sci. Rep. **3**, 2213 (2013).

[11] K. Liu, Z.-Y. Lu, and T. Xiang, Phys. Rev. B **85**, 235123 (2012).

[12] H.-Y. Cao, S. Tan, H. Xiang, D. L. Feng, and X.-G. Gong, Phys. Rev. B **89**, 014501 (2014).

[13] S. Grimme, J. Comput. Chem. **27**, 1787 (2006).

[14] A. Tkatchenko and M. Scheffler, Phys. Rev. Lett. **102**, 073005 (2009).

[15] M. Dion, H. Rydberg, E. Schröder, D. C. Langreth, and B. I. Lundqvist, Phys. Rev. Lett. **92**, 246401 (2004).

[16] K. Lee, E. D. Murray, L. Kong, B. I. Lundqvist, and D. C. Langreth, Phys. Rev. B **82**, 081101 (2010).

[17] J. Klimeš, D. R. Bowler, and A. Michaelides, Phys. Rev. B **83**, 195131 (2011).

[18] Q.-Y. Wang, Z. Li, W.-H. Zhang, Z.-C. Zhang, J.-S. Zhang, W. Li, H. Ding, Y.-B. Ou, P. Deng, K. Chang, J. Wen, C.-L. Song, K. He, J.-F. Jia, S.-H. Ji, Y.-Y. Wang, L.-L. Wang, X. Chen, X.-C. Ma, and Q.-K. Xue, Chin. Phys. Lett. **29**, 037402 (2012).

[19] Y.-Y. Xiang, F. Wang, D. Wang, Q.-H. Wang, and D.-H. Lee, Phys. Rev. B **86**, 134508 (2012).

[20] S. Tan, Y. Zhang, M. Xia, Z. Ye, F. Chen, X. Xie, R. Peng, D. Xu, Q. Fan, H. Xu, J. Jiang, T. Zhang, X. Lai, T. Xiang, J. Hu, B. Xie, and D. Feng, Nat. Mater. **12**, 634 (2013).

[21] R. Peng, X. P. Shen, X. Xie, H. C. Xu, S. Y. Tan, M. Xia, T. Zhang, H. Y. Cao, X. G. Gong, J. P. Hu, B. P. Xie, and D. L. Feng, Phys. Rev. Lett. **112**, 107001 (2014).

[22] J. J. Lee, F. T. Schmitt, R. G. Moore, S. Johnston, Y.-T. Cui, W. Li, M. Yi, Z. K. Liu, M. Hashimoto, Y. Zhang, D. H. Lu, T. P. Devereaux, D.-H. Lee, and Z.-X. Shen, Nature **515**, 245 (2014).

[23] Y. Sun, W. Zhang, Y. Xing, F. Li, Y. Zhao, Z. Xia, L. Wang, X. Ma, Q.-K. Xue, and J. Wang, Sci. Rep. **4** (2014).

[24] D. Huang, C.-L. Song, T. A. Webb, S. Fang, C.-Z. Chang, J. S. Moodera, E. Kaxiras, and J. E. Hoffman, Phys. Rev. Lett. **115**, 017002 (2015).

[25] R. Zacharia, H. Ulbricht, and T. Hertel, Phys. Rev. B **69**, 155406 (2004).

[26] W. Siemons, G. Koster, H. Yamamoto, W. A. Harrison, G. Lucovsky, T. H. Geballe, D. H. A. Blank, and M. R.

Beasley, Phys. Rev. Lett. **98**, 196802 (2007).
[27] J. Bang, Z. Li, Y. Y. Sun, A. Samanta, Y. Y. Zhang, W. Zhang, L. Wang, X. Chen, X. Ma, Q.-K. Xue, and S. B. Zhang, Phys. Rev. B **87**, 220503 (2013).
[28] Y. P. Wu, D. Zhao, X. R. Lian, X. F. Lu, N. Z. Wang, X. G. Luo, X. H. Chen, and T. Wu, Phys. Rev. B **91**, 125107 (2015).
[29] F. Ma, W. Ji, J. Hu, Z.-Y. Lu, and T. Xiang, Phys. Rev. Lett. **102**, 177003 (2009).